Available online at www.sciencedirect.com
ScienceDirect
Journal of Colloid and Interface Science 314 (2007) 615–620
JOURNAL OF Colloid and Interface Science
www.elsevier.com/locate/jcis

Controllable superhydrophobic and lipophobic properties of ordered pore indium oxide array films

Yue Li *, Guotao Duan, Weiping Cai

[a] *Ningbo Institute of Materials Technology and Engineering, Chinese Academy of Sciences (CAS), Ningbo City 315040, Zhejiang, PR China*
[b] *Key Lab of Materials Physics, Institute of Solid State Physics, Chinese Academy of Sciences, Hefei 230031, Anhui, PR China*

Received 8 March 2007; accepted 22 May 2007
Available online 31 May 2007

Abstract

Using the polystyrene (PS) colloidal monolayers as templates, ordered indium oxide pore array films with different morphologies were prepared by sol-dipping method. These porous films took on hydrophilicity, however, after chemical modification, such pore array films displayed both superhydrophobicity and lipophobicity due to rough surface and low surface free energy materials on their surfaces. Interestingly, with increase of the pore size in the films, the superhydrophobicity could be controlled and was gradually enhanced due to the corresponding increase of roughness caused by nanogaps produced by the thermal stress in the annealing process with increase of film thickness.

Keywords: Superhydrophobic; Lipophobic; Indium oxide; Macropore array film; Nanogaps

1. Introduction

Surface wettability is an important index depending on two factors: the chemical property and the geometrical micro- or nanostructure of surface materials. Superhydrophobic (water contact angle >150°) and lipophobic surfaces have many applications in fundamental research and practical uses, including self-cleaning surfaces, the prevention of the adhesion of snow, fog, raindrops and other contamination to antennas and windows, antioxidation, microfluidic devices, etc. [1–3]. The *lotus effect*, a self-cleaning effect of the lotus leaf reveals that such property is attributed to both the enough roughness and low free energy materials on its surface [4,5]. Based on these facts, various techniques have been developed to fabricate the superhydrophobic surfaces, such as a rough polymer surface by argon plasma etching [6], a hierarchical micro/nanostructured film by the wet chemical method [7], ZnO films by chemical vapor deposition [8], a binary structure by colloidal assembly [9], and a transparent boehmite/silica film by sublimation [10], superhydrophobic rough surfaces by electrochemical deposition [11], polymer patterns by the polymerization on the etched silicon substrate [12], stable bionic superhydrophobic surfaces by solution-immersion process [13] and porous films by electron irradiation or template techniques [14]. Generally, the fluorocarbon compounds, low surface free energy materials, are introduced to make material surfaces water or oil repellent. Using the fluorocarbon compounds, several superhydrophobic and lipophobic surfaces have been prepared, including rough polymer films [15], a carbon nanotube film [16], an anodically oxidized aluminum surface [17], etc. In this work, the morphologies of indium oxide macropore array films by sol-dipping colloidal monolayer template method significantly changed and became much rougher with increase of pore size. After chemically modified by a kind of fluoroalkylsilane, we found superhydrophobic and lipophobic properties of such pore array films. Importantly, the superhydrophobicity can be well controlled by changing the periodicities of colloidal monolayers and the superhydrophobicity increases with increase of sphere size.

2. Experiments

Ordinary glass or silicon substrates were ultrasonically cleaned in acetone and then in ethanol for 1 h, polystyrene sphere (PS) (4.5, 2.0 and 1.0 μm in diameter) suspensions

* Corresponding author.
E-mail address: yueli@issp.ac.cn (Y. Li).

0021-9797/$ – see front matter
doi:10.1016/j.jcis.2007.05.061

(2.5 wt% in water, surfactant-free) were purchased from Alfa Aesar Company and standard deviation of the diameter for the PSs with different sizes is less than 5%). The colloidal monolayer with a large area of 1 cm^2 was fabricated on the cleaned substrate by spin coating on a custom-built spin coater [18]. The monolayer colloidal crystals were formed based on self-assembly process induced by a capillary force between neighboring PSs on the substrate with a smooth and hydrophilic surface. The preparation of indium oxide pore array films was described as following. Briefly, the $In(OH)_3$ precursor sols were prepared by following steps: $NH_3{\cdot}H_2O$ solution was added into the 0.5 M $InCl_3$ solution slowly until the $In(OH)_3$ precipitated completely. The $In(OH)_3$ precipitate was rinsed several times with Millipore water until all Cl^- ions were removed. A certain amount of the $In(OH)_3$ powder was dispersed in 0.25 M nitric acid and its pH value was controlled at 2.4–2.5 by gradually adding $NH_3{\cdot}H_2O$ solution [19]. We thus obtained stable, homogeneous, and translucent precursor sols and average sol particle size was 23 nm determined by TEM. A droplet of precursor sol was then dropped onto the colloidal monolayer, which could infiltrate into the interstices between the substrate and the colloidal monolayer, followed by drying at 110 °C and ultrasonically washing in methylene chloride (CH_2Cl_2) for 2 min to remove the template. Finally, the sample is annealed in air at 400 °C for 1 h for the decomposition of $In(OH)_3$ into In_2O_3.

For chemical modification with low surface free energy materials, the as-prepared samples were immersed in a methanol solution of 1.0 wt% (heptadecafluoro-1,1,2,2-tetrahydrodecyl) triethoxysilane (ABCR GmbH & Co., KG, Germany) (molecular formula: $CF_3(CF_2)_7(CH_2)_2Si(OCH_2CH_3)_3$) for 8 h and subsequently dried at 50 °C for 30 min.

The synthesized samples were characterized by field emission scanning electronic microscopy (FE-SEM) (JEOL 6700). X-ray diffraction (XRD) was performed on a Philips X'Pert using the Cu$K\alpha$ line (0.15419 nm). Transmission electron microscopy (TEM, JEM-200CX) was used to measure the precursor sol particle size. The X-ray photoelectron spectrum (XPS) was characterized by an Escalabmk2 spectrophotometer. The static CAs of the water were measured on a homebuilt contact angle meter at room temperature. The weight of the water droplets used for the static CA measurements was 5 mg. The values of the CAs were obtained by averages of five measurements made on different areas of the sample surface.

3. Results and discussion

Using the PS colloidal monolayers as templates, the ordered macropore array films could be fabricated on the substrate after removal of the PSs and annealing at 400 °C in air for 1 h. Fig. 1 shows the FE-SEM images of macropore array films prepared using the colloidal monolayer with different PS sphere sizes ((a) 1; (c) 2; (e) 4.5 μm). The XRD pattern indicates that such pore array films are composed of indium oxide crystal with body-centered cubic structure (see Fig. 2). We can see that macropores exhibit the orderly hexagonal arrangement, which corresponds well to the colloidal monolayer template.

When the diameter of PS sphere is 1 μm in the colloidal monolayer, by the sol-dipping method, after removal of PS sphere template and annealing at 400 °C for 1 h, honeycomb structured, ordered indium oxide macropore array films with hexagonal alignment are formed, as shown in Figs. 1a and 1b. If the size of PS sphere increases to 2 μm, indium oxide pore array film also can be formed and pore shapes are close to hollow hemispheres (Figs. 1c and 1d). However, most walls between the two neighboring pores cracked and many nanogaps were produced, which could be clearly observed in the magnified image (Fig. 1d). Further increasing the PS sphere size to 4.5 μm, we find that the macropore shapes were seriously deformed and changed from hollow hemisphere shape to irregular shape. Additionally, many nanogaps with big size were also produced on the walls between the two neighboring pores, as shown in Figs. 1e and 1f.

Generally, thermal stress will be produced in the annealing process of film materials. With increase of the film thickness, the influence of thermal stress on the film morphology is becoming more serious, especially for the rupture behavior of film. In our case, with increase of PS sphere size in the colloidal monolayer template, the thickness of macropore array film fabricated using such template will correspondingly increase. With PS sphere size is relatively small (1 μm), the height or thickness of pore array film is about half of sphere size and the thermal stress nearly has no influence on pore array films in the annealing process at 400 °C for 1 h, so the morphology of the pore array film correspond perfectly to that of the colloidal monolayer template and exhibit hexagonally arranged regular pore. However, when a colloidal monolayer with PS sphere diameter of 2 μm is used as a template and the thickness of pore array film correspondingly increases, the thermal stress begins to play an important role in formation of pore array film and leads that many nanogaps are produced on the pore walls. If the thickness of pore film is increased further by the colloidal template with sphere size of 4.5 μm, influence of thermal stress become more serious, resulting in the deformed pore shapes and nanogaps on the pore wall.

In addition, for the pore array film, it belongs to a kind of rough surface in essence. According to our results, we can clearly see that roughness of pore array film increased with increase of the PS sphere size in the colloidal monolayer template due to the effect of thermal stress.

After chemical modification with fluoroalkylsilane, the surface chemical composition of pore array film can be characterized by X-ray photoelectron spectroscopy (XPS). The XPS spectra of the as prepared sample indicate that the sample is composed of the elements of silicon, carbon, fluorine, oxygen and indium, as displayed in Fig. 3. The indium and partial oxygen originate from the indium oxide pore array films. The other elements of silicon, carbon, fluorine and small part of oxygen come from (heptadecafluoro-1,1,2,2-tetrahydrodecyl) triethoxysilane. The XPS spectra indicate the low surface free energy material (fluoroalkylsilane) has been effectively introduced on the indium oxide pore array films.

The wettability of as prepared samples was evaluated by the water contact angle (CA) measurement. Before modified with

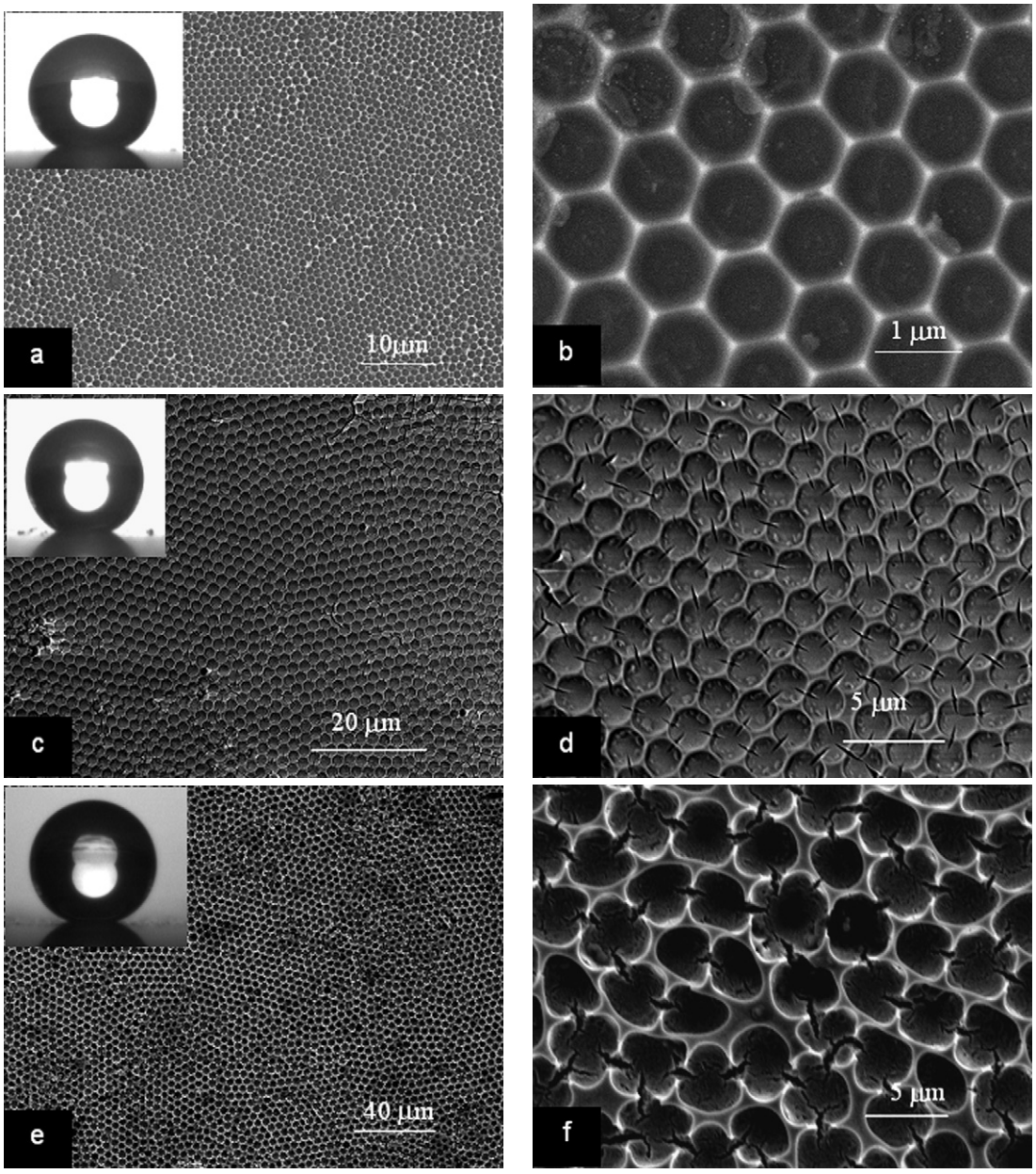

Fig. 1. FE SEM image of indium oxide pore array films after removal of the PS sphere and annealing at 400 °C, based on the colloidal monolayer templates by sol-dipping method. The diameter the PS sphere in the colloidal monolayer: (a–b) 1, (c–d) 2, (e–f) 4.5 μm. The images of (b), (d) and (f) are the magnification of (a), (c) and (e), respectively. The precursor concentration: (a) 0.2, (c) 0.4, (e) 05 M. The insets in (a), (c) and (d) are photographs of the water droplet shapes on corresponding pore arrays after chemical modifications with fluoroalkylsilane and corresponding water contact angle are 155°, 158° and 163°, respectively.

fluoroalkylsilane, all samples took on the hydrophilicity (water CA <90°) and the water CA decreased with increase of pore size, as shown in curve b in Fig. 4. Surprisingly, after modified with fluoroalkylsilane, the morphologies of such ordered pore arrays were nearly unchanged, however, the wettability was changed from the original hydrophilicity to superhydrophobicity. Moreover, with increase of the pore size from 1 μm, to 2 μm and finally to 4.5 μm, the water contact angle increased from 155°, 158° and 163°, respectively, as shown in curve b in Fig. 4. Additionally, the water droplet on them was gradually close to spherical shape with increase of pore size in the films, as shown in insets in Figs. 1a, 1c and 1e, reflecting that the superhydrophobicity was enhanced with increase of pore size. Our results indicate that the superhydrophobicity can be well controlled by change the periodicities of colloidal templates.

Generally, the wettability of a certain material is closely associated with its roughness on its surface. For the rough surfaces, Wenzel presented a model describing the water dewetting behavior on porous films as following [20],

$$\cos\theta r = r\cos\theta, \tag{1}$$

where r is the roughness factor, which is the ratio of total surface area to the projected area on the horizontal plane, and θr and θ are the CAs on a porous film and a native film with smooth surface, respectively. For a Wenzel type surface, obviously, high roughness can enhance both hydrophobicity of

hydrophobic surface and hydrophilicity of hydrophilic surface. The θ value, a relative flat indium oxide film prepared by dip-coating method without using colloidal monolayer template, was 85°, indicating that the wettability of a flat film is hydrophilic. In our work, these indium oxide pore array films are

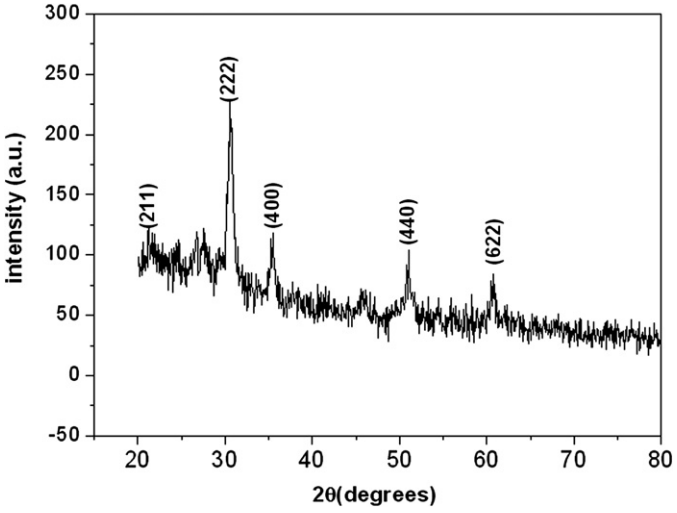

Fig. 2. XRD spectrum of the ordered pore array film annealing at 400 °C corresponding to the sample in Fig. 1a. The marked indices correspond well to indium oxide crystals.

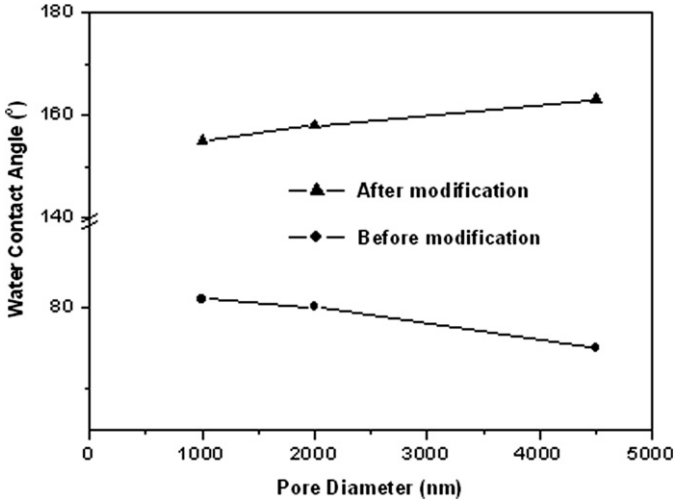

Fig. 4. Curves of water contact angles on indium oxide pore array films with different pore size before and after modified with fluoroalkylsilane.

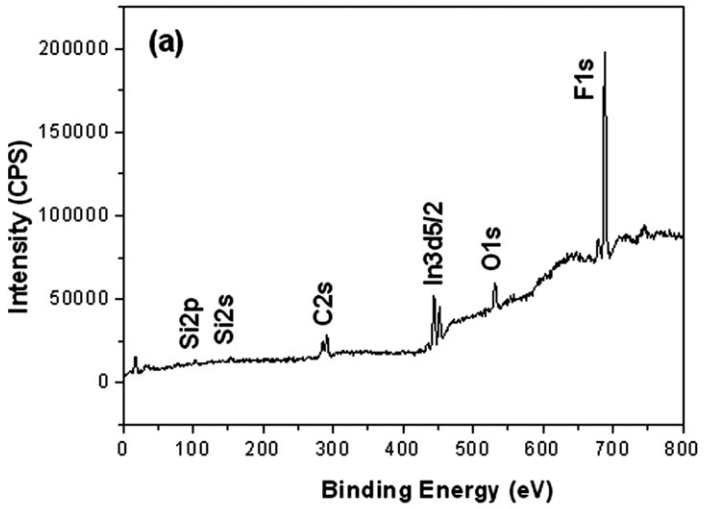

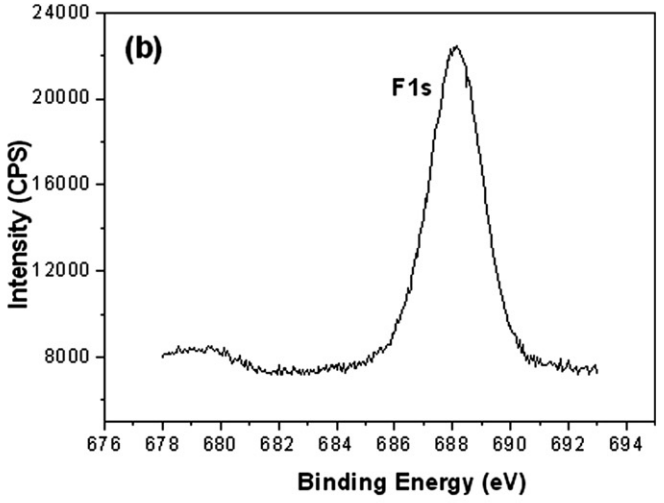

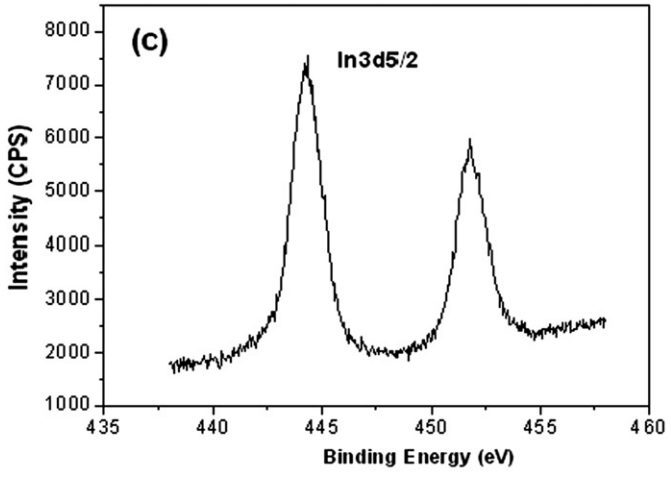

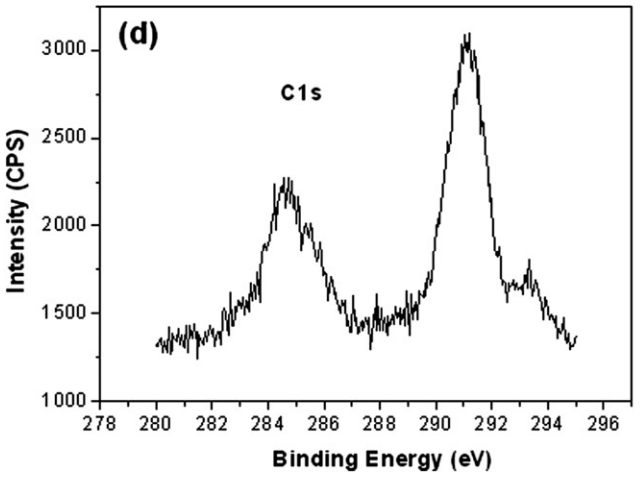

Fig. 3. XPS spectra of the indium oxide pore array films modified with fluoroalkylsilane (a); (b), (c) and (d) are corresponding XPS spectra of F1s, In3d5/2 and C1s, respectively.

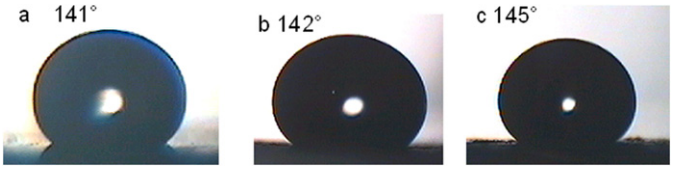

Fig. 5. The photographs of rapeseed oil droplet on the indium oxide pore array films after modification. Pore size: 1, 2, 4.5 μm for (a), (b) and (c), respectively.

much rougher than the relative flat surface, and the roughness of pore array films increases with increase of pore size duo to many nanogaps produced on the pore walls as mentioned above. So the Wenzel model can well explain why such pore array films exhibit hydrophilicity and the hydrophilicity was enhanced with increase of pore size. Additionally, the relative flat indium oxide film displayed the hydrophobicity with water CA of 115° after chemical modification. According to Wenzel model, for the same reason, the indium oxide pore films are so rougher that the hydrophobicity is enhanced to water superrepellence and all such films displayed the superhydrophobicity. The superhydrophobicity increases with increase of pore size due to corresponding increase of roughness.

For the pore film with high roughness obtained by the colloidal template with PS size of 4.5 μm, air can be trapped in pore or nanogaps on pore walls at the films. In this case, Cassie and Baxter presented a model to describe the wettability as following [21]:

$$\cos\theta_r = f_1 \cos\theta - f_2, \tag{2}$$

where f_1 is the area fraction of a water droplet in contact with a pore film, and $f_2 = 1 - f_1$ is the area fraction of a water droplet in contact with air on such a surface. Because the water CAs of a relative flat indium oxide surface and the pore film modified with fluoroalkylsilane are 115° and 163°, respectively, f_2 is calculated to be 0.93. This indicates that such pore film produces a large amount of air traps in macropores and nanogaps in pore walls, and hence, a strong superhydrophobicity could be induced.

Interestingly, such indium oxide pore array films exhibited not only water repellence but also oil repellence after chemical modification by low surface free energy materials. The rape oil, a kind of lipophilic solvent, displayed contact angles larger than 140° for these porous film and lipophobicity increase with increase of pore size controlled by the colloidal monolayer with different periodicities, as shown in Fig. 5.

4. Conclusions

In conclusion, large-scale ordered macropore indium oxide array films were synthesized based on colloidal monolayer templates and the sol-dipping method. Such pore array films exhibited both water superrepellence and oil repellence after chemical modification. And their superhydrophobicity could be well controlled by changing the periodicities of colloidal templates Additionally, because the superhydrophobic surface consists of ordered pore structured array, the whole surface has uniform superhydrophobicity and lipophobicity. Such pore array films have potential applications in microreactor, microseparator and microfluidic devices.

Acknowledgments

This work was supported by the Ningbo Natural Science Foundation (Grant No. 2006A610060), Zhejiang Provincial Natural Science Foundation of China (Grant No. Y405136), the National Natural Science Foundation of China (Grant Nos. 50601026, 50671100) and Anhui Provincial Natural Science Foundation of China (Grant No. 070414199).

References

[1] P. Ball, Nature 400 (1999) 507.
[2] A. Nakajima, K. Hashimoto, T. Watanabe, Monatsh. Chem. 132 (2001) 31.
[3] Z.-Z. Gu, H. Uetsuka, K. Takahashi, R. Nakajima, H. Onishi, A. Fujishima, O. Sato, Angew. Chem. Int. Ed. 42 (2003) 894.
[4] (a) W. Barthlott, C. Neinhuis, Planta 202 (1997) 1;
(b) C. Neinhuis, W. Barthlott, Ann. Bot. 79 (1997) 667;
(c) R. Blossey, Nat. Mater. 2 (2003) 301.
[5] (a) X. Gao, L. Jiang, Nature 432 (2004) 36;
(b) L. Feng, S. Li, Y. Li, H. Li, L. Zhang, J. Zhai, Y. Song, B. Liu, L. Jiang, D. Zhu, Adv. Mater. 14 (2002) 1857;
(c) T. Sun, L. Feng, X. Feng, L. Jiang, Acc. Chem. Res. 38 (2005) 644.
[6] W. Chen, A. Fadeev, M. Hsieh, D. Öner, J. Youngblood, T. McCarthy, Langmuir 15 (1999) 3395.
[7] Y. Li, X.J. Huang, S.H. Heo, C.C. Li, Y.K. Choi, W.P. Cai, S.O. Cho, Langmuir 23 (2007) 2169.
[8] H. Liu, L. Feng, J. Zhai, L. Jiang, D. Zhu, Langmuir 20 (2004) 5659.
[9] (a) G. Zhang, D.Y. Wang, Z.-Z. Gu, H. Möhwald, Langmuir 21 (2005) 9143;
(b) W. Ming, D. Wu, R. van Benthem, G. de With, Nano Lett. 5 (2005) 2298.
[10] A. Nakajima, A. Fujishima, K. Hashimoto, T. Watanabe, Adv. Mater. 11 (1999) 1365.
[11] (a) M. Nicolas, F. Guittard, S. Géribaldi, Langmuir 22 (2006) 3081;
(b) X. Zhang, F. Shi, X. Yu, H. Liu, Y. Fu, Z. Wang, L. Jiang, X. Li, J. Am. Chem. Soc. 126 (2004) 3064;
(c) L. Zhang, Z. Zhou, B. Cheng, J.M. DeSimone, E.T. Samulski, Langmuir 22 (2006) 8576.
[12] F. Xia, L. Feng, S. Wang, T. Sun, W. Song, W. Jiang, L. Jiang, Adv. Mater. 18 (2006) 432.
[13] S. Wang, L. Feng, L. Jiang, Adv. Mater. 18 (2006) 767.
[14] (a) E.J. Lee, H.M. Lee, Y. Li, L.Y. Hong, D.P. Kim, S.O. Cho, Macromol. Rapid Commun. 28 (2007) 246;
(b) Y. Li, W.P. Cai, B.Q. Cao, G.T. Duan, F.Q. Sun, C.C. Li, L.C. Jia, Nanotechnology 17 (2006) 238;
(c) Y. Li, W.P. Cai, G.T. Duan, B.Q. Cao, F.Q. Sun, F. Lu, J. Colloid Interface Sci. 287 (2005) 634.
[15] (a) H. Yabu, M. Takebayashi, M. Tanaka, M. Shimomura, Langmuir 21 (2005) 3235;
(b) Q.D. Xie, J. Xu, L. Feng, L. Jiang, W.H. Tang, X.D. Luo, C.C. Han, Adv. Mater. 16 (2004) 302.
[16] H.J. Li, X.B. Wang, Y.L. Song, Y.Q. Liu, Q.S. Li, L. Jiang, D.B. Zhu, Angew. Chem. Int. Ed. 40 (2001) 1743.
[17] S. Shibuichi, T. Yamamoto, T. Onda, K. Tsujii, J. Colloid Interface Sci. 208 (1998) 287.
[18] (a) Y. Li, W.P. Cai, G.T. Duan, B.Q. Cao, F.Q. Sun, J. Mater. Res. 20 (2005) 338;
(b) Y. Li, W.P. Cai, B.Q. Cao, G.T. Duan, C.C. Li, F.Q. Sun, H.B. Zeng, J. Mater. Chem. 16 (2006) 609;

(c) Y. Li, W.P. Cai, B.Q. Cao, G.T. Duan, F.Q. Sun, Polymer 46 (2005) 12033;
(d) G.T. Duan, W.P. Cai, Y. Li, Z.G. Li, B.Q. Cao, Y.Y. Luo, J. Phys. Chem. B 110 (2006) 7184.
[19] Y. Li, W. Cai, G. Duan, F. Sun, B. Cao, F. Lu, Q. Fang, I.W. Boyd, Appl. Phys. A 81 (2005) 269.
[20] R.N. Wenzel, J. Phys. Colloid Chem. 53 (1949) 1446.
[21] A.B.D. Cassie, Discuss. Faraday Soc. 3 (1948) 11.